

---

# Thermally induced effects in the optical absorption of pure and doped $\text{Bi}_{12}\text{SiO}_{20}$ single crystals

Panchenko T. V. and Trubitsyn M. P.

Institute for Energy Efficient Technologies and Materials Sciences, Oles Honchar Dnipro National University, Gagarin Ave. 72, 49045, Dnipro, Ukraine  
e-mail: panchtv141@gmail.com

**Received:** 26.05.2023

**Abstract.** We study the optical absorption spectra for pure  $\text{Bi}_{12}\text{SiO}_{20}$  single crystals and the crystals doped with Cr and Mn ions. These spectra are measured in the photon-energy region 1.3–2.6 eV at the temperatures 300–670 K. The intrinsic defects with significantly different optical and thermal activation energies (respectively 1.493 and 0.66 eV) are revealed in  $\text{Bi}_{12}\text{SiO}_{20}$ . The strengths  $S$  of electron–phonon interactions at the intra-centre transitions in Cr and Mn ions are determined. We obtain  $S \approx 3.33$  (at 300 K) and 3.42 (at 420 K) for  $\text{Bi}_{12}\text{SiO}_{20}:\text{Cr}$ , as well as  $S \approx 5.26$  (at 300 K) and 5.46 (at 420 K) for  $\text{Bi}_{12}\text{SiO}_{20}:\text{Mn}$ . A significant thermochromic effect is detected in  $\text{Bi}_{12}\text{SiO}_{20}:\text{Cr}$  crystals.

**Keywords:** optical absorption spectra, thermally induced effects, sillenite crystals  $\text{Bi}_{12}\text{SiO}_{20}$ , doping Cr and Mn ions

**UDC:** 537.311.1

## 1. Introduction

Photorefractive and electro-optic sillenites with a general formula  $\text{Bi}_{12}\text{MO}_{20}$  ( $M = \text{Si}, \text{Ge}, \text{Ti}$ ) abbreviated hereafter as BMO have found many applications. They are used as active media in various devices of optical and functional electronics. In particular,  $\text{Bi}_{12}\text{SiO}_{20}$  crystals (BSO in short) are good for holographic interferometry, dynamic holography, spatiotemporal light modulation and optical waveguides or switches [1, 2].

Doping is one of the most effective ways for targeted modification of crystal properties. The photoelectric and optical properties of nominally pure and doped BMO crystals have been repeatedly studied at  $T \leq 300$  K with different experimental methods. For example, it has been shown that doping of BSO with Al and Ga ions leads to a sharp decrease in its optical absorption, whereas doping with Cr and Mn ions results in appearance of intense intra-centre absorption bands in the visible optical range [3].

Recently, many research groups have examined the temperature changes in the physical properties of BMO, which occur in the range of ‘moderately high’ temperatures ( $300 \text{ K} < T < 600 \text{ K}$ ) [4–8]. The appropriate information is important for evaluating thermal stability of the physical properties of BMO and studying possible thermally induced effects in it. For instance, the temperature regions where the piezoelectric coefficients of BSO and  $\text{Bi}_{12}\text{TiO}_{20}$  (BTO) crystals are stable have been established in Ref. [4]. The authors [5] have shown that heating of Co-doped  $\text{Bi}_{12}\text{GeO}_{20}$  (BGO) crystals up to 500 K leads to a considerable increase in its dielectric permittivity. Temperature dependences of the photorefractive effect in BGO have been studied in Ref. [6]. Stationary and irradiation-induced optical absorption in BTO doped with Zn and Ca and BSO has been revealed [7]. Moreover, a thermochromic effect (TCE) has been

observed in Al- and Ga-doped BSO crystals [8]. A notable role of temperature in the relaxation dynamics of charge carriers in Cr-doped BSO crystals has also been indicated [9].

It is obvious that further studies of temperature influence on the optical properties of BSO can enable obtaining new functional materials with required characteristics. Temperature dependences of the optical absorption due to the transitions of a ‘deep level–conduction zone (or valence zone)’ type have been analyzed in our previous work [10]. The main attention has been paid to the levels with the optical activation energies 1.65 eV (BSO and BSO:Cr crystals) and 1.68 eV (BSO:Mn crystals).

The purpose of the present work is to study the influence of temperature on the intense optical absorption due to intra-centre electronic transitions in doping Cr and Mn ions. In addition, it would be interesting to investigate the temperature dependences of the absorption associated with some other deep levels in the BSO crystals and consider a possibility for exciting the TCE.

Considering the BSO crystals and the dopants under study, one should consider that recording of holograms by light pulses is accompanied by appearance of a photorefractive lattice and, additionally, a photochromic lattice [11]. Moreover, it is known that the Cr and Mn dopants enhance notably the photochromic effect (PCE) in BSO [12].

## 2. Experiments

Single crystals of BSO, BSO:Cr and BSO:Mn were grown by a Czochralski method along the crystallographic direction [001]. In accordance with our spectral-emission analysis, the impurity contents in the doped crystals amounted to 0.02 mass % for Cr and 0.3 mass % for Mn. The samples were prepared in the shape of polished plates with the thicknesses  $d = 3\text{--}5$  mm and the dimensions  $8 \times 8$  mm<sup>2</sup> of the main planes (001).

The spectra of the stationary optical transmittance  $t_0(h\nu, T_0)$  and the transmittances detected in the processes of heating ( $t^{T^+}(h\nu, T)$ ) and cooling ( $t^{T^-}(h\nu, T)$ ) were recorded with a Specord M40 spectrophotometer. The measurements were performed in the range of light-quantum energies  $h\nu = 1.3\text{--}2.6$  eV. The temperature of the samples was changed in both heating and cooling cycles in the range 300–670 K, with the rate of 0.625 K/min. The samples were kept for 10 min at the maximal temperature,  $T = 670$  K, and then cooled down. Intense long-wavelength bands associated with the intra-centre absorption of Cr and Mn ions are located in the spectral range under test. These bands are hardly distorted by a possible superposition with the weak absorption bands arising from the intrinsic defects of BSO crystal matrix. This is in contrast to the short-wavelength bands falling into the region of ‘defect-absorption shoulder’ ( $h\nu = 2.5\text{--}3.3$  eV), which is adjacent to the edge of fundamental absorption in BSO [12].

We studied the spectra  $\alpha_0(h\nu, T_0)$  of the stationary absorption measured at a fixed temperature, as well as the absorptions  $\alpha^{T^+}(h\nu, T)$  and  $\alpha^{T^-}(h\nu, T)$  recorded respectively on heating and cooling. Moreover, we determined the spectral changes  $\Delta\alpha^{TCE}(h\nu, T_0) = \alpha^{T^-}(h\nu, T_0) - \alpha_0(h\nu, T_0)$  occurring after a heating–cooling cycle, which characterizes the TCE. The temperature dependences of the impurity-driven absorption bands  $\alpha_m^{T^+}(T)$  and  $\alpha_m^{\uparrow}(T^-)(T)$  were determined from the parametric dependences  $\alpha^{T^+}(h\nu, T)$  and  $\alpha^{T^-}(h\nu, T)$ . The absorption spectra themselves were calculated using a method described earlier in Ref. [12].

## 3. Results and discussion

The effect of temperature on the optical absorption of our crystals is illustrated in Fig. 1. The BSO crystals have two weak absorption bands located at  $h\nu_{\max 1} = 1.493$  eV and  $h\nu_{\max 2} = 1.767$  eV. The intensities of these bands decrease on heating, although their spectral positions do not change.

Moreover, the edge absorption increases under this condition. This absorption is caused by the electronic transitions into the conduction band and the so-called ‘Urbach tail’, which is associated with the energy states of shallow levels located near the ceiling of the valence band. The relevant absorption undergoes a long-wavelength shift.

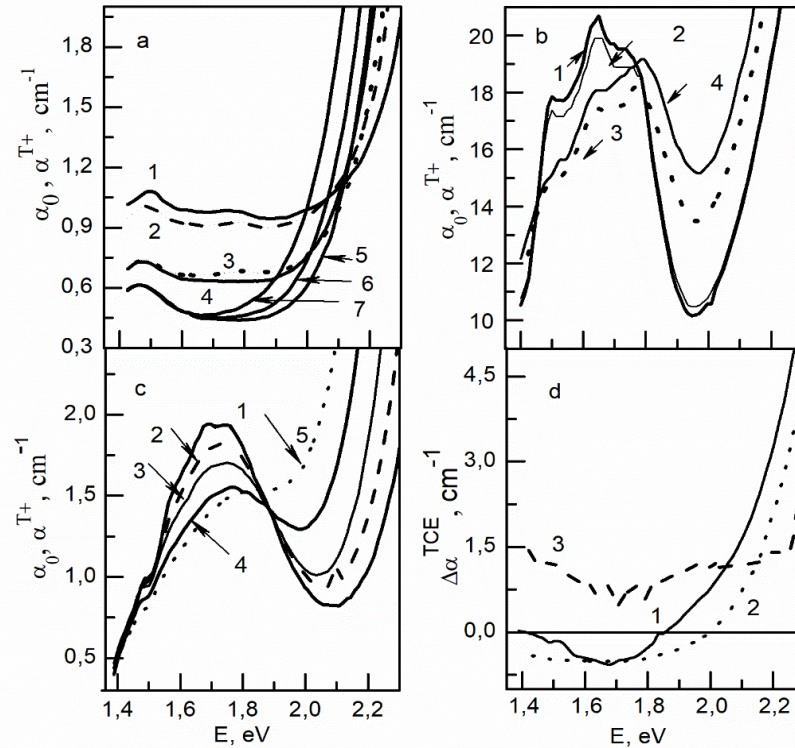


**Fig.1.** Temperature variations of optical absorption spectra in BSO (a), BSO:Cr (b) and BSO:Mn (c), and TCE-induced absorption (d): (a)  $\alpha^{T+}(h\nu)$  spectra for BSO at  $T = 300$  (curve 1), 323 (curve 2), 373 (curve 3), 423 (curve 4), 473 (curve 5), 523 (curve 6) and 573 K (curve 7); (b)  $\alpha^{T+}(h\nu)$  spectra for BSO:Cr at  $T = 300$  (1), 323 (2), 423 (3) and 523 K (4); (c)  $\alpha^{T+}(h\nu)$  spectra for BSO:Mn at  $T = 300$  (1), 323 (2), 373 (3), 423 (4) and 523 K (5); (d) TCE spectra  $\Delta\alpha^{TCE}(h\nu, T_0)$  for undoped BSO (1), BSO:Mn (2) and BSO:Cr (3).

The band located at  $h\nu_{\max 2}$  is suppressed by the edge absorption at  $T \geq 400$  K (see Fig. 1a). As the temperature increases, the intensities of both bands decrease non-monotonically. The  $\alpha_m^{T+}(T)$  dependences for the band located at  $h\nu_{\max 1}$  show two ‘steps’ of sharp absorption drop. On subsequent cooling, the intensity of the band located at  $h\nu_{\max 1}$  does not recover (see Fig. 2a). The less intense band located at  $h\nu_{\max 2}$  shows a similar behaviour on cooling. However, the situation changes in the interval  $h\nu \approx 1.8\text{--}2.1$  eV: the dependences  $\alpha_m^{T+}(T)$  come through a minimum at  $\sim 530$  K and then show an increasing trend (see Fig. 2b, curve 1). On subsequent cooling, the  $\alpha_m^{T-}(T)$  dependences demonstrate a significant decrease (see Fig. 2b, curve 2). This is due to competition of the processes of emptying levels with the optical activation energy  $E_{\alpha 2}^0 > 1.767$  eV and filling with electrons of the levels located near the ceiling of the valence band, which form the ‘Urbach tail’.

Let us recall that a photoconductivity peak in BSO has been observed in this spectral range at the room temperature [13]. Then we assume that the bands located at  $h\nu_{\max 1}$  and  $h\nu_{\max 2}$  are caused by the transitions of electrons from the local levels into the conduction band, respectively with the

optical activation energies  $E_{\alpha_1}^0 = 1.493$  eV and  $E_{\alpha_2}^0 = 1.767$  eV. The electrons fall down to the levels in the Urbach tail of states from the conduction band. Earlier, we have shown [10, 14] that the similar dependences  $\alpha_m^{T+}(T)$  can be used to determine the thermal activation energy  $E_{\alpha}^T$  of the electronic transitions. This is because the temperature dependences of their temperature derivative  $d\alpha_m^{T+}(T)/dT$  taken with the negative sign are similar to the temperature dependences of a thermally stimulated current [15]. Indeed, our dependence  $d\alpha_m^{T+}(T)/dT$  obtained for the band with the peak  $h\nu_{\max 1}$  shows two peaks located at  $T_{\max 1} \approx 400$  K and  $T_{\max 2} \approx 500$  K (see Fig. 2a).

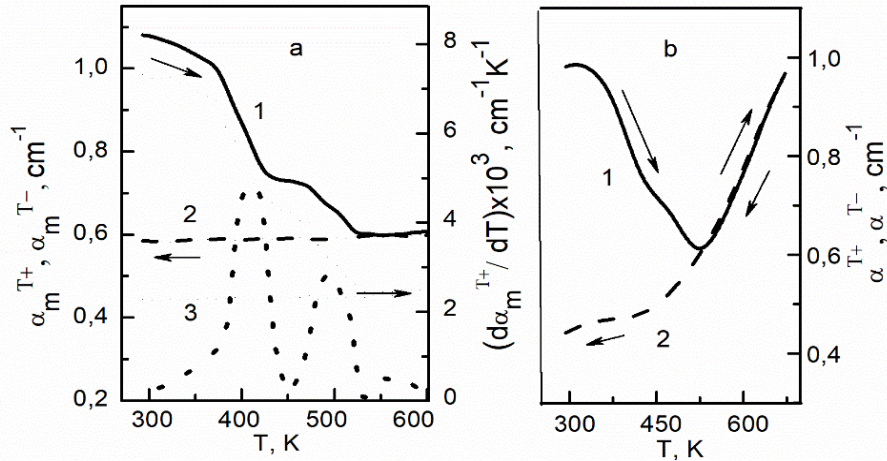


**Fig. 2.** Temperature dependences  $\alpha_m^{T+}(T)$  (curve 1),  $\alpha_m^{T-}(T)$  (curve 2) and  $d\alpha_m^{T+}(T)/dT$  (curve 3) for the absorption band in BSO centred at  $h\nu_{\max 1} = 1.493$  eV (panel a); temperature dependences  $\alpha^{T+}(h\nu, T)$  (curve 1) and  $\alpha^{T-}(h\nu, T)$  (curve 2) at  $h\nu = 1.9$  eV detected in BSO on cooling (panel b).

The temperature positions of these peaks correspond to the positions of the thermally-stimulated current peaks detected in the BSO crystals [15]. The energy  $E_{\alpha_1}^T = 0.66$  eV for the peak at  $T_{\max 1}$  can be found by an ‘initial slope’ method. Then the value  $E_{\alpha_2}^0 = 0.86$  eV for the peak at  $T_{\max 2}$  can be calculated from the relation  $E_{\alpha_2}^0 = AkT_{\max 2}$  [note that the coefficient  $A = 20$  has been found in Ref. [15]]. Both  $E_{\alpha}^T$  values correlate with those determined from the corresponding thermally-stimulated current peaks [15]. Earlier, a similar difference in the energies  $E_{\alpha}^0$  and  $E_{\alpha}^T$  has been detected for the electronic transitions of a type ‘impurity level–(conduction or valence) zone’ in Al-doped BSO crystals [16]. Finally, a significant difference in the  $E_{\alpha}^0$  and  $E_{\alpha}^T$  energies evidences for a strong electron–phonon interaction existing in the BSO crystals.

A presence of the spectral interval  $\Delta h\nu = 1.8$ – $2.1$  eV where, upon heating, the regime of crystal ‘brightening’ below the temperature  $T_{cr} = 530$  K changes to the regime of its ‘darkening’ at  $T \geq 530$  K represents a peculiar feature of the  $\alpha_m^{T+}(T)$  dependences found in the BSO crystals (see Fig. 2b, curve 1). This effect is not observed upon subsequent cooling (see Fig. 2b, curve 2). The TCE in the BSO crystals is negative. In other words, the difference in the spectra, which is observed at  $T_0$  before and after the heating–cooling cycle, results in a so-called ‘lumen band’ (see Fig. 1d).

The intra-centre absorption bands of Cr and Mn ions in BSO:Cr and BSO:Mn are broadened and structured. They can be represented by envelopes of several narrow components (see Fig. 1b and Fig. 1c). These bands are defined as  $U$ -bands from the group of three broad  $U$ -,  $Y$ -, and  $V$ -

bands characteristic of the same type of  $d-d$  transitions in  $\text{Cr}^{3+}$  and  $\text{Mn}^{4+}$  ions with the  $3d^3$  iso-electronic configuration to which the quartet terms  ${}^2A_4$ ,  ${}^2T_4$ ,  ${}^2A_4$ ,  $a^2T_1$ ,  $b^2T_1$  belong [12]. This corresponds to a short-wavelength shift of the main  $U$ -band components in  $\text{Mn}^{4+}$  ions ( $\Delta h\nu \approx 0.04$  eV) relative to those in  $\text{Cr}^{3+}$  ions (see Fig. 1b and Fig. 1c). According to the crystal-field theory, this shift can be attributed to increasing charge of the impurity ions.

In both BSO:Mn and BSO:Cr crystals, the  $U$ -band broadens with increasing temperature, decreases in its intensity and shifts towards the short-wavelength side (see Fig. 1b and Fig. 1c). This temperature behaviour indicates a strong electron–phonon interaction for the electronic transitions in the  $U$ -band from the orbital singlet  ${}^2A_4(t_2^3)$  to the triplet  ${}^2T_4(t_2^3, {}^3T_{1,c})$ . The Huang–Reese parameter  $S$ , which characterizes the strength of electron–phonon interaction with the optical vibrations of BSO lattice, can be approximately found from the relation  $\Delta h\nu^* = \sqrt{2S} h\Omega_0$ , where  $\Delta h\nu^*$  is the half-width of the  $U$ -bands and  $\Omega_0$  the frequency of the effective longitudinal optical phonons [17]. By decomposing the broad structured absorption bands due to Cr and Mn ions into Gaussians components, one can determine  $\Delta h\nu^*$  for the main and the most intense components, which are characterized by  $h\nu_{\max} = 1.646$  eV (Cr) and  $h\nu_{\max} = 1.689$  eV (Mn).

Assuming that  $\text{Cr}^{3+}$  and  $\text{Mn}^{4+}$  impurity ions replace for  $\text{Bi}^{3+}$  hosts located within oxygen octahedrons [12], we use the frequency  $\Omega_0 = 500 \text{ cm}^{-1}$  corresponding to the vibrations of Bi–O valence bonds [18]. Then we obtain  $S_1 = 3.33$  (BSO:Cr) and  $S_2 = 5.26$  (BSO:Mn) at  $T_0$ . A temperature increase enhances the electron–phonon interaction, so that one obtains  $S_1 = 3.42$  (BSO:Cr) and  $S_2 = 5.46$  (BSO:Mn) at  $T = 420$  K.

For a comparison, one can determine the  $S^*$  values for the electronic transitions of the ‘impurity-zone’ type described above for the BSO crystals. From the relation  $E_\alpha^0 - E_\alpha^T = Sh\Omega_0$  suggested in the frame of a configuration coordinates model [17], we obtain  $S_1^* = 13.23$  and  $S_2^* = 17.37$  for the levels with  $E_{\alpha_1}^0 = 1.493$  eV and  $E_{\alpha_2}^0 = 1.767$  eV, respectively. These  $S_1^*$  and  $S_2^*$  values fall within the range of values  $S^* = 1, 2, \dots, 20$  obtained for the other crystals [17].

The temperature dependences of intensities of the main  $U$ -band components  $\alpha_m^{T+}(T)$  and  $\alpha_m^{T-}(T)$  for the BSO:Mn and BSO:Cr crystals are significantly different (cf. Fig. 3a and Fig. 3b).

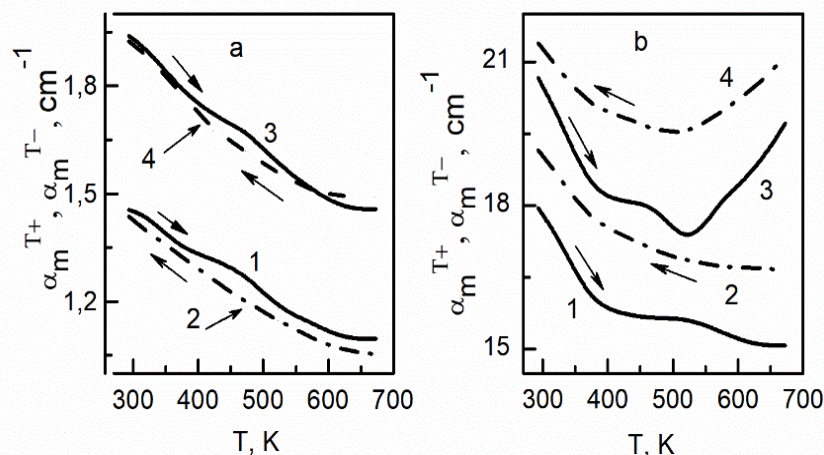


**Fig. 3.** Temperature dependences  $\alpha_m^{T+}(T)$  (curves 1 and 3) and  $\alpha_m^{T-}(T)$  (curves 2 and 4) for the absorption bands located at  $h\nu_{\max} = 1.562$  eV (curves 1 and 2) and  $1.686$  eV (curves 3 and 4) in BSO:Mn (panel a). Temperature dependences  $\alpha_m^{T+}(T)$  (1, 3) and  $\alpha_m^{T-}(T)$  (2, 4) for the absorption bands located at  $h\nu_{\max} = 1.502$  eV (1, 2) and  $1.649$  eV (3, 4) in BSO:Cr (panel b).

For BSO:Mn, they reveal a nearly exponential decrease on heating, with the activation energies  $E_{\alpha}^{Mn} = 0.019$  and  $0.014$  eV referred respectively to the components located at  $h\nu_{\max} = 1.564$  and  $1.684$  eV. On cooling, a small ‘negative’ hysteresis is observed, i.e. a ‘backward’ absorption is less than the ‘forward’ one (see Fig. 3a). For BSO:Cr, the  $\alpha_m^{T+}(T)$  dependence for the component with  $h\nu_{\max} = 1.646$  eV passes through a minimum at  $T_{cr} \approx 530$  K.

A significant ‘positive’ hysteresis is observed for BSO:Cr. Here the absorption increases after the heating–cooling cycle. There is no return to the initial absorption values at  $T_0$  (see Fig. 3b), which indicates the appearance of the TCE. The  $\alpha_m^{T-}(T)$  dependence found for the component with  $h\nu_{\max} = 1.496$  eV is close to exponential, with  $E_{\alpha}^{Cr} = 0.005$  eV.

Such dependences can be explained when assuming that Cr ions create some local levels filled with electrons inside the BSO bandgap. These levels become depleted on heating, and the electrons move to empty levels inside the Urbach tail. The Urbach absorption in BSO increases, overlaps with the  $U$ -band absorption by Cr ions and amplifies it. This behaviour also explains the TCE spectra shown in Fig. 1d.

#### 4. Conclusions

1. Local levels of the intrinsic defects with different optical and thermal activation energies have been detected inside the bandgap of the undoped BSO crystals. Their thermal depletion is accompanied by the effect of ‘brightening’ of the crystal that goes to the temperature  $T_{cr} \approx 450$  K from below. The ‘brightening’ changes to its opposite, so that the samples of undoped BSO are ‘darkening’ on heating above 450 K.

2. The manifestations of electron–phonon interactions for the intra-centre transitions in Cr and Mn ions have been considered. The interaction strength (i.e., the Huang-Reese factor) has been determined. We have  $S \approx 3.33$  at 300 K and 3.42 at 420 K for BSO:Cr. The same parameters for BSO:Mn are equal to  $S \approx 5.26$  at 300 K and 5.46 at 420 K. It has been shown that the factor  $S$  increases on heating.

3. A weak ‘negative’ TCE effect resulting in crystal ‘brightening’ has been found for undoped BSO and BSO:Mn. On the other hand, a significant ‘positive’ TCE (i.e., a crystal ‘darkening’) has been observed for the BSO:Cr crystals.

**Funding.** This work was supported by the Ministry of Education and Science of Ukraine under the Grant 0122U001228.

**Disclosures.** The authors declare no conflicts of interest.

#### References

1. Gunter P and Huignard J. Photorefractive Materials and Their Applications. Part 1. New York: Springer Science + Business Media, 2006.
2. Gesualdi M R R, Barbosa E A and Muramatsu M, 2006. Advances in phase-stepping real-time holography using photorefractive sillenite crystals, *J. Optoelectron. Adv. Mater.* **8**: 1574–1583.
3. Panchenko T V and Truseyeva N A, 1984. Optical absorption in doped  $\text{Bi}_{12}\text{SiO}_{20}$  crystals. *Ukr. J. Phys.* **29**: 1186–1191.
4. Shen Chuanying, Zhang Huaijin, Zhang Yuanyuan, Xu Honghao, Yu Haohai, Wang Jiyang and Zhang Shujun, 2014. Orientation and temperature dependence of piezoelectric properties for sillenite-type  $\text{Bi}_{12}\text{TiO}_{20}$  and  $\text{Bi}_{12}\text{SiO}_{20}$  single crystals. *Crystals.* **4**: 141–151.

5. Filipič C, Klos A, Gajc M, Pawlak D A, Dolinšek J and Levstik A, 2015. Dielectric relaxation in pure and Co-doped  $\text{Bi}_{12}\text{GeO}_{20}$  single crystals. *J. Adv. Dielect.* **5**: 1550023.
6. Foldvari I, Martin J J, Hunt C A, Powell R C, Reeves R J and Agnes P, 1993. Temperature dependence of the photorefractive effect in undoped  $\text{Bi}_{12}\text{GeO}_{20}$ . *J. Appl. Phys.* **74**: 783–788.
7. Shandarov S M, Polyakova L E, Mandel A E, Kisteneva M G, Vidal J, Kargin Yu F and Egorysheva A V, 2007. Temperature dependences of optical absorption and its light-induced changes in crystals sillenite. *Proc. SPIE.* **6595**: 124–131.
8. Dyachenko A O and Panchenko T V, 2018. Thermochromic effect in doped  $\text{Bi}_{12}\text{SiO}_{20}$  crystals. *Acta Phys. Polon. A.* **133**: 936–939.
9. Wubetu G A, Marinova V and Goovaerts E, 2021. Optical study of relaxation dynamics of photo-induced absorption of Cr-doped  $\text{Bi}_{12}\text{SiO}_{20}$  crystals. *Physica B.* **608**: 412778.
10. Panchenko T V, 1998. Thermo-optical investigation of deep levels in doped  $\text{Bi}_{12}\text{SiO}_{20}$  crystals. *Phys. Sol. State.* **40**: 452–457.
11. Khromov A L, Kamshilin A A and Petrov M P, 1990. Photochromic and photorefractive gratings induced by pulsed excitation in BSO crystals. *Opt. Commun.* **77**: 139–143.
12. Panchenko T V and Truseyeva N A, 1991. Optical absorption and photochromic effect in Cr and Mn doped  $\text{Bi}_{12}\text{SiO}_{20}$  single crystals. *Ferroelectrics.* **115**: 73–80.
13. Panchenko T V and Yanchuk Z Z, 1996. Photoelectric properties of  $\text{Bi}_{12}\text{SiO}_{20}$  crystals. *Physics of the Solid State.* **38**: 1113–1118.
14. Panchenko T and Karpova L, 2020. Thermally activated spectroscopy of optical absorption in  $\text{Bi}_{12}\text{SiO}_{20}$  crystals. *Ukr. J. Phys. Opt.* **21**: 84–92.
15. Panchenko T V and Snezhnoy G V, 1994. Polarization effects of undoped and Al, Ga-doped  $\text{Bi}_{12}\text{SiO}_{20}$  crystals. *Ferroelectrics.* **155**: 103–108.
16. Briat B, Panchenko T V, Rjeilly H Bou and Hamri A, 1998. Optical and magneto-optical characterization of the Al acceptor levels in  $\text{Bi}_{12}\text{SiO}_{20}$ . *J. Opt. Soc. Amer. B.* **15**: 2147–2153.
17. Ridley B K. *Quantum processes in semiconductors*. Oxford: Clarendon Press, 1982.
18. Wojdowski W, 1985. Vibration modes in  $\text{Bi}_{12}\text{GeO}_{20}$  and  $\text{Bi}_{12}\text{SiO}_{20}$  crystals. *Phys. Stat. Sol. (b).* **130**: 121–130.

---

Panchenko T. V. and Trubitsyn M. P. 2023. Thermally induced effects in the optical absorption of pure and doped  $\text{Bi}_{12}\text{SiO}_{20}$  single crystals. *Ukr. J. Phys. Opt.* 24: 04001 – 04007.  
doi: 10.3116/16091833/24/4/04001/2023

**Анотація.** Досліджено спектри оптичного поглинання чистих монокристалів  $\text{Bi}_{12}\text{SiO}_{20}$  і цих же кристалів, легованих йонами Cr і Mn. Спектри виміряно в області енергій фотонів 1,3–2,6 eV за температур 300–670 K. У кристалах  $\text{Bi}_{12}\text{SiO}_{20}$  виявлено власні дефекти із суттєво різними оптичними та термічними енергіями активації (відповідно 1,493 і 0,66 eV). Визначено сили  $S$  електрон-фононої взаємодії при внутрішньоцентрових переходах у йонах Cr і Mn. Одержано  $S \approx 3,33$  (при 300 K) і 3,42 (при 420 K) для  $\text{Bi}_{12}\text{SiO}_{20}:\text{Cr}$ , а також  $S \approx 5,26$  (при 300 K) і 5,46 (при 420 K) для  $\text{Bi}_{12}\text{SiO}_{20}:\text{Mn}$ . У кристалах  $\text{Bi}_{12}\text{SiO}_{20}:\text{Cr}$  виявлено значний термохромний ефект.

**Ключові слова:** спектри оптичного поглинання, термоіндуковані ефекти, кристали силеніту  $\text{Bi}_{12}\text{SiO}_{20}$ , легуючі Cr і Mn іони.